Supplementary material

Effects of layer thickness and annealing process on low-frequency noise and detectivity in tunnel magnetoresistive sensors with CoFeSiB soft magnetic layers

Murali Krishnan M., Prabhanjan D. Kulkarni, Tomoya Nakatani,* Hirofumi Suto, and Yuya Sakuraba

Research Center for Magnetic and Spintronic Materials, National Institute for Materials Science, 1-2-1, Sengen, Tsukuba, Ibaraki 305-0047, Japan,

* Corresponding author. Email: nakatani.tomoya@nims.go.jp

1. Resistance–magnetic field (*R–H*) curves

Figure S1 shows the *R–H* curves of the TMR devices used in this study. The device size was 60 μm in diameter. The values of resistance-area product in the P-state (RA_P) are given in the table of each figure. Note that the variations in RA_P of these devices were not only due to the annealing process and t_{CFSB} variations but also due to the non-uniformity of the thickness of the MgO tunnel barrier on each device, which was unavoidable in our deposition apparatus. Therefore, we do not have a sufficient experimental precision to discuss the relationships between RA_P and the annealing process/t_{CFSB}.

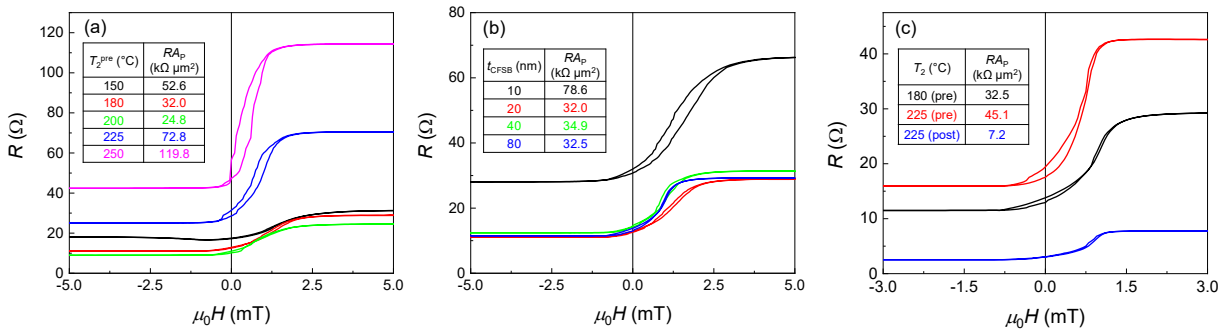

FIG. S1. *R–H* curves of the TMR devices with variations in (a) the temperature of the second pre-fabrication annealing (T_2^{pre}) for with t_{CFSB} = 20 nm, (b) t_{CFSB} for T_2^{pre} = 180 °C, and (c) T_2 condition for t_{CFSB} = 80 nm. (a), (b), and (c) correspond to Figs. 2, 3, and 4, respectively.

2. Coercivity and noise

In Figure S2, we show the H dependence of the coercivity (H_c) of the R-H curve, the noise voltage spectral densities at f = 10 Hz, and the sensitivity for the TMR devices annealed at T_2^{pre} = 180 and 225 °C and T_2^{post} = 225 °C. For all devices, the maximum H_c was observed at $\mu_0 H \sim 0$ mT, whereas the noise showed a peak at $\mu_0 H \sim 1$ mT. Therefore, H_c and the noise did not show a clear correlation. On the other hand, the noise showed a clear correlation with the sensitivity as discussed in the main text of this paper.

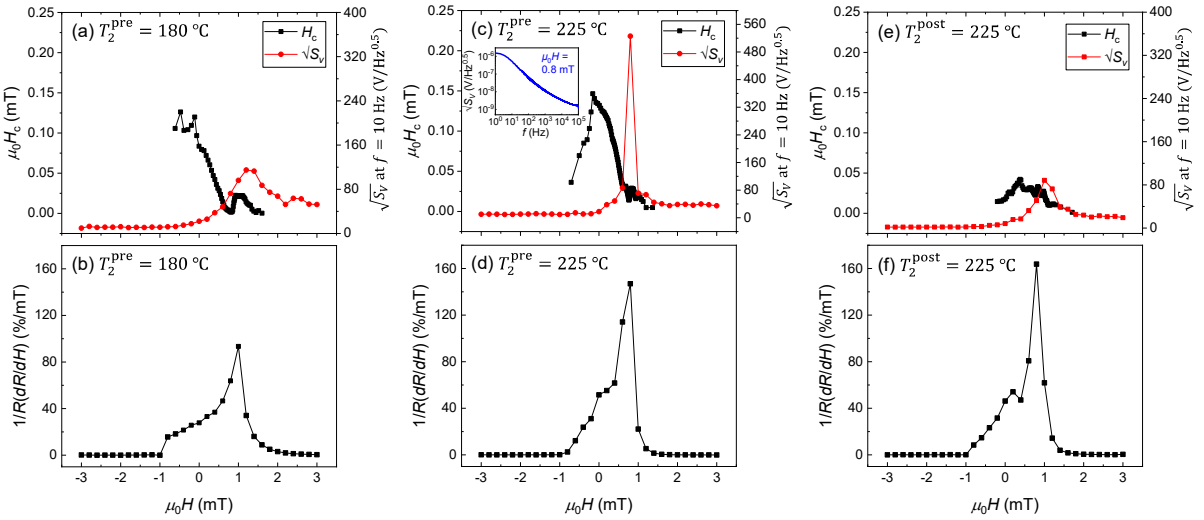

FIG. S2. *H*-dependences of (a), (c), and (e) coercivity (H_c) of the *R*-*H* curves and the noise voltage spectral densities ($\sqrt{S_V}$) at *f* = 10 Hz and (b), (d), and (f) sensitivities of the TMR samples processed at T_2^{pre} = 180 and 225 °C and T_2^{post} = 225 °C, respectively. The large $\sqrt{S_V}$ at $\mu_0 H$ = 0.8 mT in (c) was by a low frequency random telegraph noise as shown in the inset.

3. Resistance-susceptibility measurements

Figure S3 shows the schematic block diagram for the resistance susceptibility (χ_R) measurement. The TMR device under test was mounted on a concentric six-turn coil fabricated on a printed circuit board (PCB). A constant current of 100 μA was applied to the TMR device using a Keithley 2450 source measure unit. The output voltage of the TMR device was measured by a phase-sensitive detection technique using a lock-in amplifier (Stanford Research Systems, SR830). The voltage across a 0.1 Ω resistor, connected in series between the bipolar

power supply and the coil, was used as the reference signal for the lock-in amplifier. An external DC magnetic field was applied along the hard axis of the free layer magnetization. An AC modulation field was generated by the six-turn coil and applied along the hard axis of the free layer. The amplitude of the modulation field was calibrated by measuring the shift in the *R*-*H* curves when a constant DC current was applied to the coil. A current of 1 A generated a 0.7 mT field at the position of the TMR device.

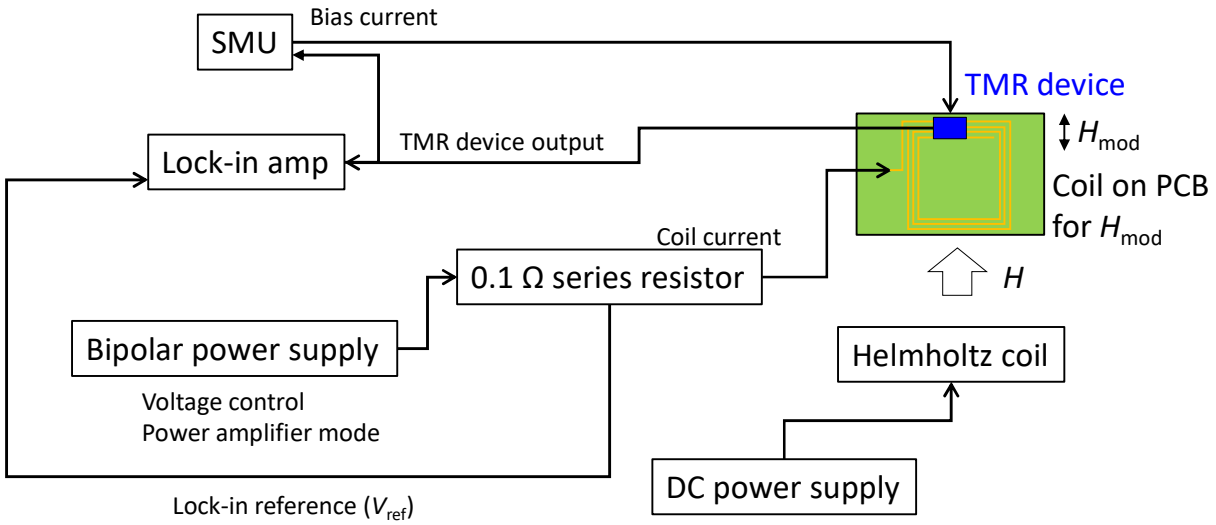

FIG. S3. Schematic block diagram for resistance susceptibility measurements.

Figures S4(a) and (b) show the H dependence of the sensitivity of the TMR devices annealed at T_2^{pre} = 225 °C and T_2^{post} = 225 °C, respectively. We compared the sensitivity measured by two types of methods: (1) the first derivative of the *R*-*H* curve normalized by R $\left(\frac{1}{R}\frac{dR}{dH}\right)$ and (2) the sensitivity obtained by the lock-in measurement with a modulation field of 0.03 mT at a frequency of 103 Hz, defined as the magnetoresistance susceptibility (χ_R/R). R is the resistance of the device, and χ_R is the resultant of the χ_R' and χ_R'' by the resistance-susceptibility measurement. The χ_R/R value deviated from the $\frac{1}{R}\frac{dR}{dH}$ value at the $\mu_0 H$ range at approximately 0.8 mT, which can be explained as follows. In the *R*-*H* full loop measurement, a Barkhausen-type jump of the magnetic domains may occur at the transition between the P and AP states. In contrast, in the χ_R measurement with a small modulation field, the free layer magnetization responds to the modulation field in magnetization rotation regime without

causing a magnetic domain jump, resulting in $\frac{\chi_R}{R} < \frac{1}{R}\frac{dR}{dH}$. For the device with T_2^{pre} = 225 °C, the highest value of χ_R/R was 60.7% of that of $\frac{1}{R}\frac{dR}{dH}$. For T_2^{post} = 225 °C, the highest value of χ_R/R was 44.1% of that of $\frac{1}{R}\frac{dR}{dH}$. This indicates that the device with T_2^{pre} = 225 °C has a more Barkhausen domain jump than that with T_2^{post} = 225 °C. Further studies are needed to understand the origin of the reduced magnetic 1/f noise by post-fabrication annealing.

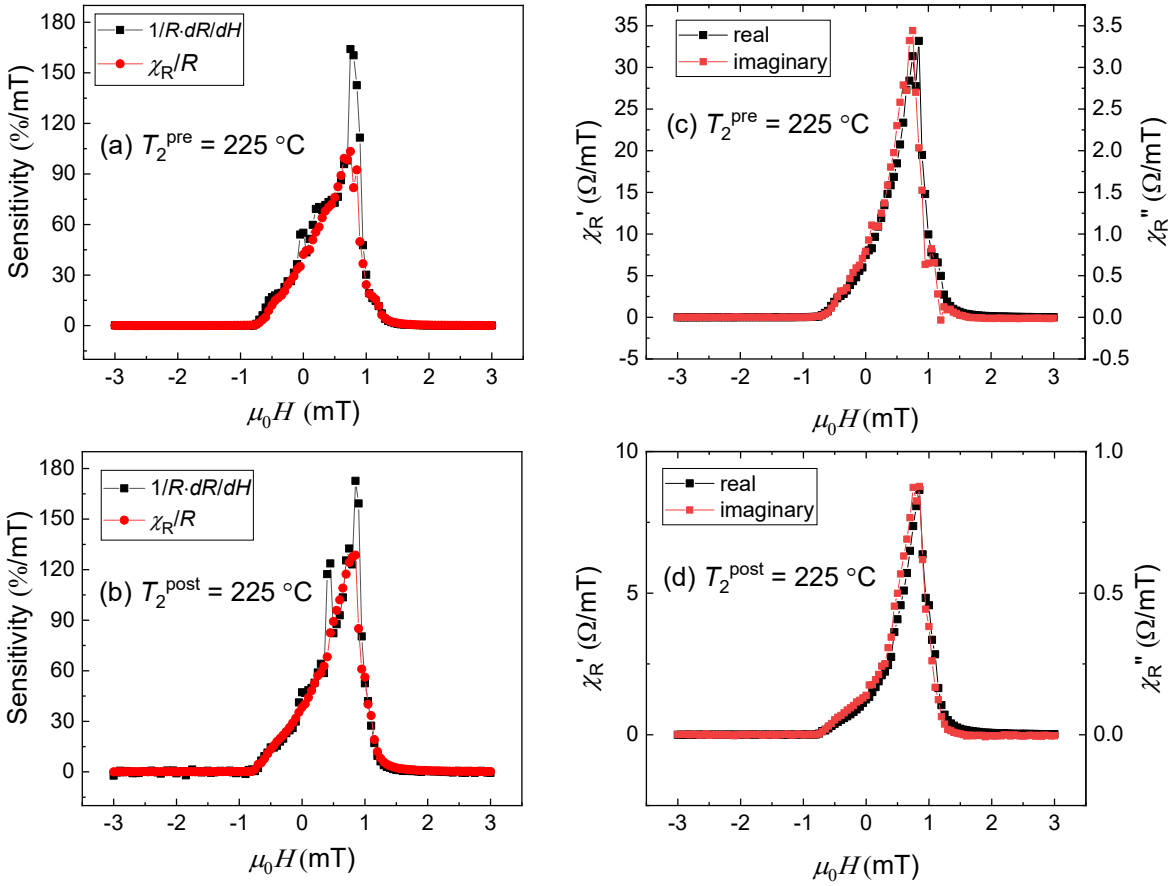

FIG. S4 (a) and (b) Sensitivity curves of the TMR devices annealed at T_2^{pre} = 225 °C and T_2^{post} = 225 °C, respectively, obtained from the R-H full loop measurements ($\frac{1}{R}\frac{dR}{dH}$) and the locking measurements with a modulation field amplitude of 0.03 mT and a frequency of 103 Hz. (c) and (d) Real (in-phase) and imaginary (out-of-phase) resistance susceptibilities for T_2^{pre} = 225 °C and T_2^{post} = 225 °C, respectively.

Figures S4(c) and (d) show the in-phase (real part, χ_R') and out-of-phase (imaginary part, χ_R'') components of the resistance susceptibility. The values of χ_R' were approximately ten times larger than those of χ_R'' in the H range where the device exhibited nonzero sensitivity. In addition, χ_R' and χ_R'' showed a similar H dependence. Figure S5 shows the H dependence of the phase lag, $\varepsilon = \tan^{-1}(\chi_R'/\chi_R'')$ at 103 Hz. The phase shift caused by the electrical cables and the electronic components was corrected from the data obtained for the TMR devices. No significant variation in the phase lag was be observed between these devices in the H range where α_H exhibited a nonlinear dependence with the magnetoresistance-sensitivity product (MSP) (Fig. 5(b)). Furthermore, no clear correlation between H_c of the R-H curve and ε can be observed when comparing Fig. S2(c, e) and Fig. 5,

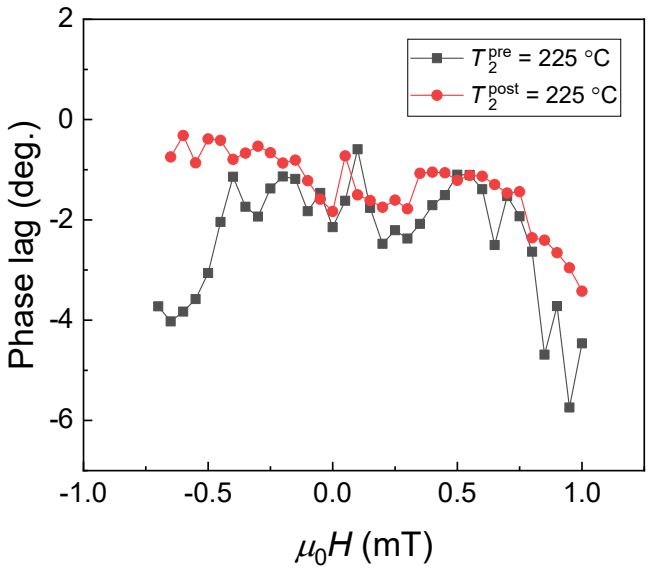

FIG. S5. Magnetic field dependence of phase lag for TMR devices annealed at T_2^{pre} = 225 °C and T_2^{post} = 225 °C.